Supplementary Materials: The Highly Conducting Spin-Crossover Compound Combining Fe(III) Cation Complex With TCNQ in a Fractional Reduction State. Synthesis, Structure, Electric and Magnetic Properties

Yuri N. Shvachko, Denis V. Starichenko, Aleksander V. Korolyov, Alexander I. Kotov, Lev I. Buravov, Vladimir N. Zverev, Sergey V. Simonov, Leokadiya V. Zorina and Eduard B. Yagubskii

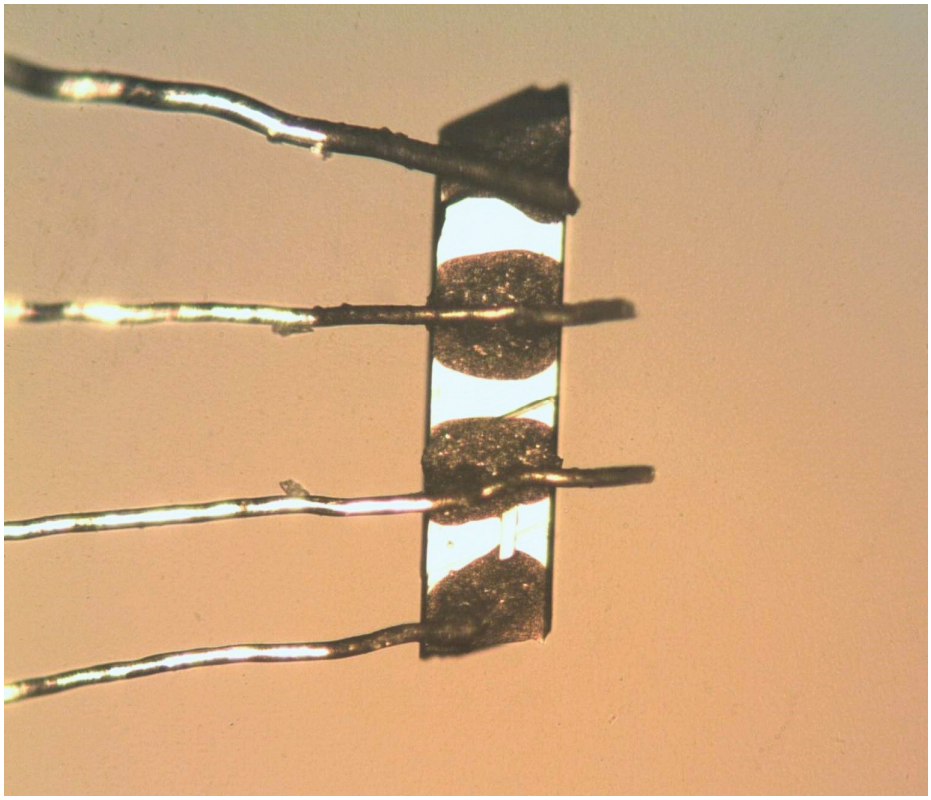

Figure S1. A crystal (size $0.6 \times 0.15 \times 0.05$ mm^3) of complex **1**·MeOH with the electrodes for measurement of conductivity.

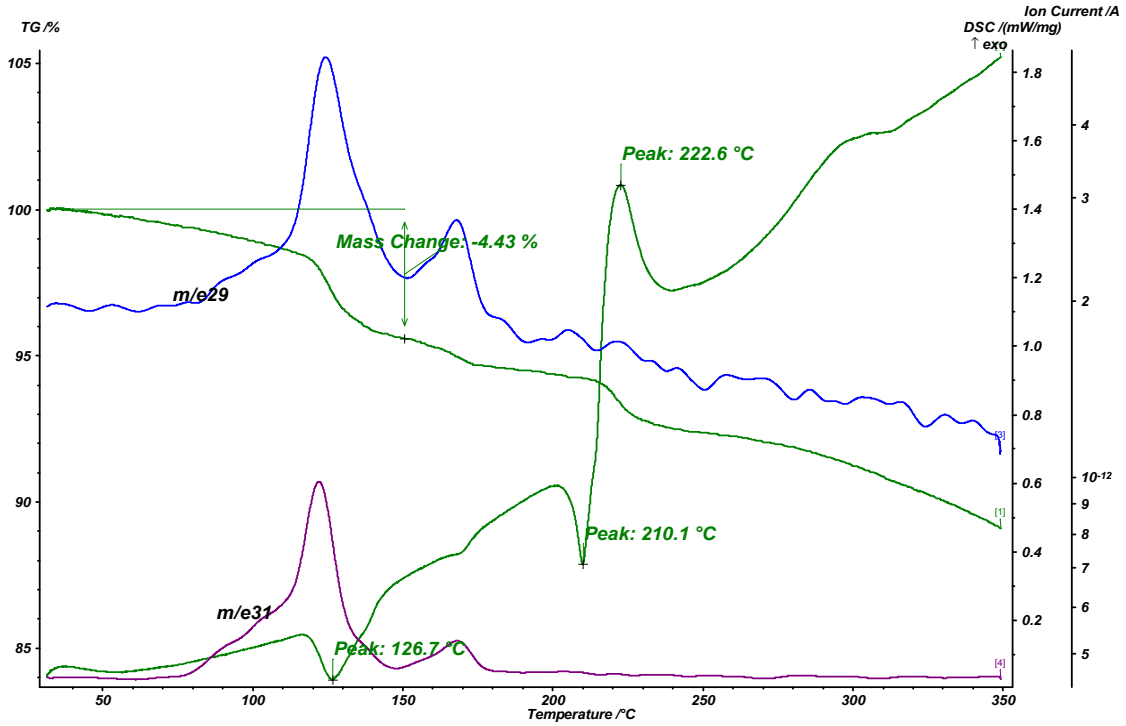

Figure S2. *TG-DSC* curves and mass spectra for 1·MeOH. Calculated mass loss for one molecule of CH_3OH 3.77 %, found 4.43%.

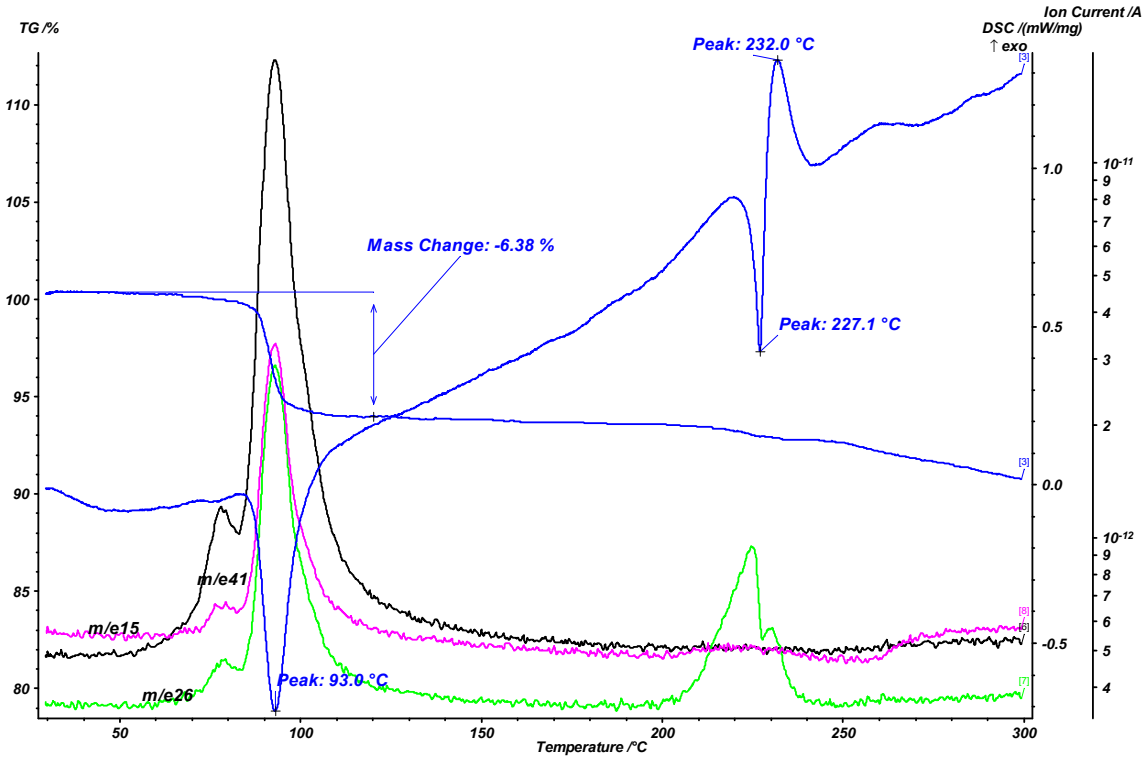

Figure S3. *TG-DSC* curves and mass spectra for **2**. Calculated mass loss for one molecule of CH_3CN 6.27 %, found 6.38%.

Table S1. The charges (δ) of TCNQ radical anions estimated from Kistenmacher's empirical formula δ = A[c/(b+d)] + B (A = −41.667, B = 19.833).

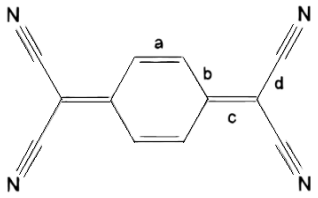

Compounds	a	b	c	d	c/(b+d)	δ(e)
$TCNQ^{0}$	1.346	1.448	1.374	1.440	0.476	0.0
$TCNQ^{-1}$	1.373	1.423	1.420	1.416	0.500	−1.0
$TCNQ^{-0.5}$	1.354	1.434	1.396	1.428	0.488	−0.5
TCNQ **I** (**1**·MeOH, 100K)	1.359	1.437	1.395	1.434	0.486	−0.41
TCNQ **II** (**1**·MeOH, 100K)	1.360	1.431	1.406	1.430	0.491	−0.64
TCNQ **I** (**1**·MeOH, 220K)	1.353	1.435	1.394	1.430	0.486	−0.43
TCNQ **II** (**1**·MeOH, 220K)	1.353	1.435	1.398	1.428	0.488	−0.51
TCNQ **I** (**1**·MeOH, 295K)	1.354	1.432	1.395	1.426	0.488	−0.50
TCNQ **II** (**1**·MeOH, 295K)	1.356	1.429	1.398	1.424	0.490	−0.58
TCNQ **I** (**1**·MeOH, 340K)	1.349	1.431	1.393	1.428	0.487	−0.47
TCNQ **II** (**1**·MeOH, 340K)	1.354	1.429	1.398	1.425	0.490	−0.58
TCNQ **I** (**1**, 350K)	1.351	1.428	1.396	1.423	0.489	−0.56
TCNQ **II** (**1**, 350K)	1.353	1.426	1.398	1.426	0.490	−0.59
TCNQ **I** (**1**, 385K)	1.342	1.429	1.395	1.424	0.489	−0.53
TCNQ **II** (**1**, 385K)	1.351	1.426	1.395	1.431	0.488	−0.52
TCNQ **I** (**1**, 325K)	1.355	1.434	1.401	1.431	0.489	−0.54
TCNQ **II** (**1**, 325K)	1.359	1.431	1.404	1.429	0.491	−0.61
TCNQ **I** (**1**, 295K)	1.356	1.437	1.399	1.433	0.487	−0.48
TCNQ **II** (**1**, 295K)	1.358	1.434	1.405	1.429	0.491	−0.61
TCNQ **I** (**1**, 260K)	1.353	1.433	1.393	1.426	0.487	−0.47
TCNQ **II** (**1**, 260K)	1.354	1.429	1.400	1.426	0.490	−0.60
TCNQ **I** (**1**, 220K)	1.354	1.439	1.394	1.431	0.486	−0.40
TCNQ **II** (**1**, 220K)	1.356	1.432	1.404	1.427	0.491	−0.62
TCNQ (**2**, 100K)	1.366	1.423	1.416	1.421	0.498	−0.91
TCNQ (**2**, 220K)	1.365	1.419	1.417	1.415	0.500	−1.00
TCNQ (**2**, 295K)	1.360	1.417	1.417	1.413	0.501	−1.04
TCNQ (**2**, 325K)	1.355	1.418	1.417	1.416	0.500	−0.99

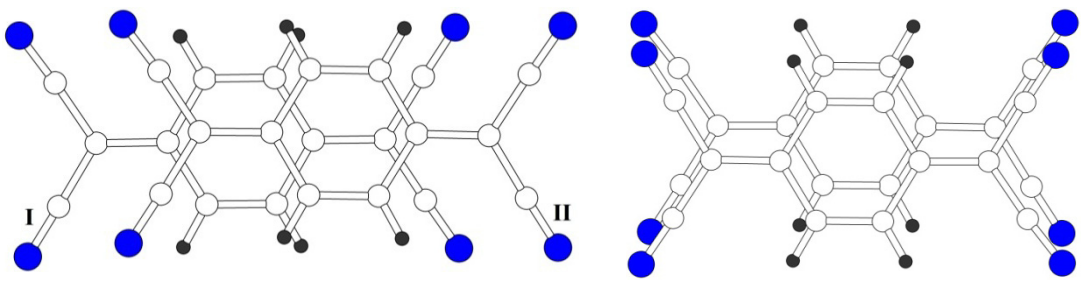

(**a**) (**b**)

Figure S4. The character of TCNQ overlap within the **II-I-I-II** tetrads (**a**) and between the tetrads (**b**) in **1**·MeOH at 100K.

Table S2. Selected bond lengths (Å) and angles (°) in **1**·MeOH and **1**.

Parameter	**1·MeOH** **100 K**	**1·MeOH** **220 K**	**1·MeOH** **295 K**	**1·MeOH** **340 K**	**1** **350 K**	**1** **385 K**	**1** **325 K**	**1** **295 K**	**1** **260 K**	**1** **220 K**
Fe1 O1	1.8775(15)	1.8744(13)	1.8697(10)	1.8678(16)	1.868(2)	1.867(2)	1.8737(18)	1.8741(15)	1.8676(14)	1.8727(11)
Fe1 O2	1.8929(15)	1.8929(12)	1.8888(9)	1.8931(16)	1.877(3)	1.890(3)	1.880(2)	1.8806(18)	1.8769(15)	1.8851(12)
Fe1 N1	1.9277(18)	1.9280(14)	1.9281(11)	1.9334(19)	1.950(3)	1.982(4)	1.936(2)	1.929(2)	1.9181(17)	1.9233(14)
Fe1 N2	1.9427(18)	1.9420(15)	1.9426(11)	1.9506(19)	1.993(2)	2.018(3)	1.976(2)	1.9595(18)	1.9448(16)	1.9449(14)
Fe1 N3	2.0052(19)	2.0023(17)	2.0062(12)	2.014(2)	2.024(3)	2.061(4)	2.018(3)	2.010(2)	1.9973(18)	2.0027(14)
Fe1 N4	2.0093(19)	2.0088(16)	2.0130(11)	2.014(2)	2.067(3)	2.100(3)	2.052(2)	2.031(2)	2.0131(18)	2.0145(15)
O1 Fe1 O2	91.43(7)	91.66(6)	91.95(4)	92.16(8)	96.28(11)	97.71(12)	95.16(9)	94.50(8)	94.14(7)	94.01(5)
O1 Fe1 N1	93.83(7)	93.88(6)	93.93(5)	93.79(8)	92.21(11)	91.25(13)	93.07(9)	93.58(8)	93.81(7)	94.01(5)
O2 Fe1 N1	89.14(7)	89.20(6)	89.44(4)	89.97(8)	92.69(13)	93.46(14)	91.79(11)	90.97(8)	90.61(7)	90.32(6)
O1 Fe1 N2	87.49(7)	87.10(6)	87.05(5)	87.27(8)	86.91(9)	87.65(11)	86.20(9)	85.67(7)	85.40(7)	85.26(5)
O2 Fe1 N2	93.13(7)	93.25(6)	93.11(4)	92.94(7)	90.83(10)	89.68(12)	91.69(9)	92.39(8)	92.65(7)	92.75(5)
N1 Fe1 N2	177.35(8)	177.34(6)	177.24(5)	176.87(8)	176.45(13)	176.79(15)	176.49(11)	176.60(9)	176.70(8)	176.89(6)
O1 Fe1 N3	176.72(8)	176.34(7)	176.14(5)	175.53(8)	172.85(12)	170.61(14)	174.69(10)	176.01(8)	176.76(7)	177.07(6)
O2 Fe1 N3	91.08(7)	91.36(6)	91.21(5)	91.39(8)	89.54(12)	89.30(14)	89.33(10)	88.83(8)	88.50(7)	88.31(6)
N1 Fe1 N3	84.10(8)	84.10(7)	83.88(5)	83.50(9)	83.34(15)	82.05(19)	83.95(12)	84.16(9)	84.27(8)	84.19(6)
N2 Fe1 N3	94.48(8)	94.79(7)	94.99(5)	95.26(9)	97.19(14)	98.69(18)	96.51(11)	96.39(9)	96.36(8)	96.42(6)
O1 Fe1 N4	92.71(7)	92.56(6)	92.35(5)	92.69(8)	93.06(11)	93.49(13)	92.87(9)	92.76(8)	92.68(7)	92.68(6)
O2 Fe1 N4	174.38(7)	174.23(6)	174.10(5)	173.37(8)	167.49(11)	164.63(12)	169.58(9)	170.90(8)	171.60(7)	171.86(5)
N1 Fe1 N4	94.36(8)	94.44(6)	94.30(5)	94.21(9)	95.26(13)	96.79(15)	94.41(11)	94.05(9)	93.84(8)	93.83(6)
N2 Fe1 N4	83.28(8)	83.04(6)	83.08(5)	82.79(9)	81.36(11)	80.28(13)	82.21(9)	82.68(8)	83.00(7)	83.19(6)
N3 Fe1 N4	84.92(8)	84.57(7)	84.66(5)	83.99(9)	81.81(13)	80.84(17)	83.01(11)	84.14(9)	84.86(8)	85.16(6)
α	53.87(6)	55.57(5)	56.71(4)	57.65(8)	64.00(11)	66.12(12)	62.93(9)	62.01(7)	61.39(6)	60.81(5)

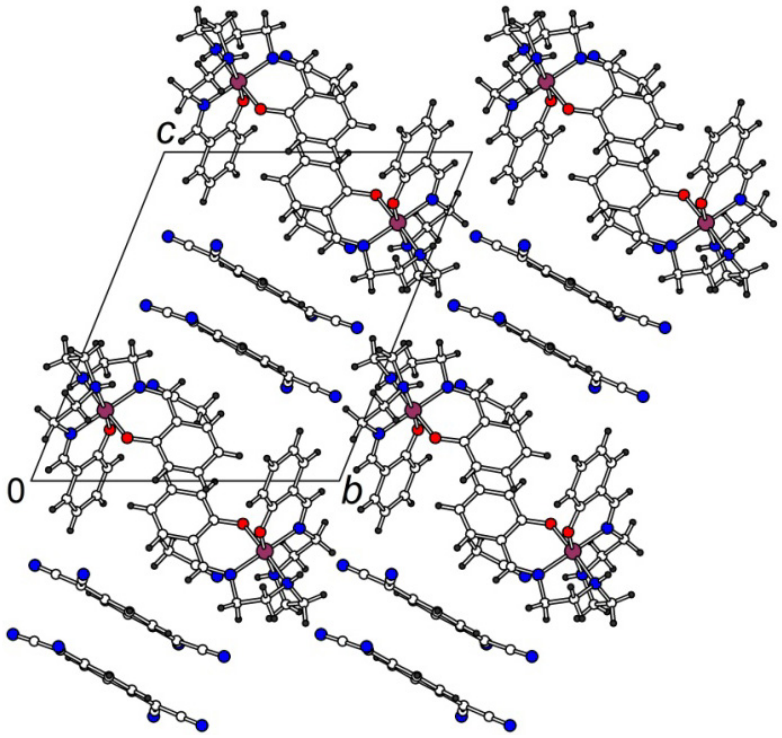

Figure S5. View of the structure **2** along *a*.

Table S3. Selected bond lengths (Å) and angles (°) in **2**.

Parameter	2 100K	2 220K	2 295K	2 325K
Fe1 O1	1.8806(12)	1.8756(9)	1.8763(10)	1.8748(12)
Fe1 O2	1.8788(12)	1.8765(10)	1.8736(11)	1.8783(11)
Fe1 N1	1.9278(15)	1.9264(11)	1.9291(12)	1.9376(15)
Fe1 N4	1.9339(15)	1.9280(12)	1.9262(14)	1.9239(16)
Fe1 N2	2.0053(15)	2.0013(12)	2.0045(13)	2.0095(15)
Fe1 N3	2.0074(15)	2.0046(12)	2.0086(14)	2.0162(15)
O1 Fe1 O2	96.23(5)	96.02(4)	96.13(5)	96.30(5)
O1 Fe1 N1	93.29(6)	93.38(4)	93.20(5)	93.00(6)
O2 Fe1 N1	87.57(6)	87.76(4)	88.03(5)	88.13(5)
O1 Fe1 N4	86.19(6)	86.37(5)	86.40(5)	86.68(6)
O2 Fe1 N4	93.60(6)	93.49(5)	93.41(5)	93.38(6)
N1 Fe1 N4	178.76(6)	178.75(5)	178.54(6)	178.48(6)
O1 Fe1 N2	174.64(6)	174.49(5)	174.03(6)	173.53(6)
O2 Fe1 N2	88.54(6)	88.88(5)	89.05(5)	89.16(6)
N1 Fe1 N2	84.44(6)	84.26(5)	84.00(6)	83.68(7)
N2 Fe1 N4	95.99(6)	95.89(5)	96.27(6)	96.49(7)
O1 Fe1 N3	90.57(6)	90.64(5)	90.71(6)	90.86(6)
O2 Fe1 N3	172.73(6)	172.89(5)	172.58(5)	172.22(6)
N1 Fe1 N3	94.62(6)	94.35(5)	94.46(6)	94.56(7)
N3 Fe1 N4	84.27(6)	84.43(5)	84.14(6)	83.96(7)
N2 Fe1 N3	84.78(6)	84.58(5)	84.27(6)	83.89(7)
α	77.23(4)	77.85(5)	78.02(5)	77.96(6)

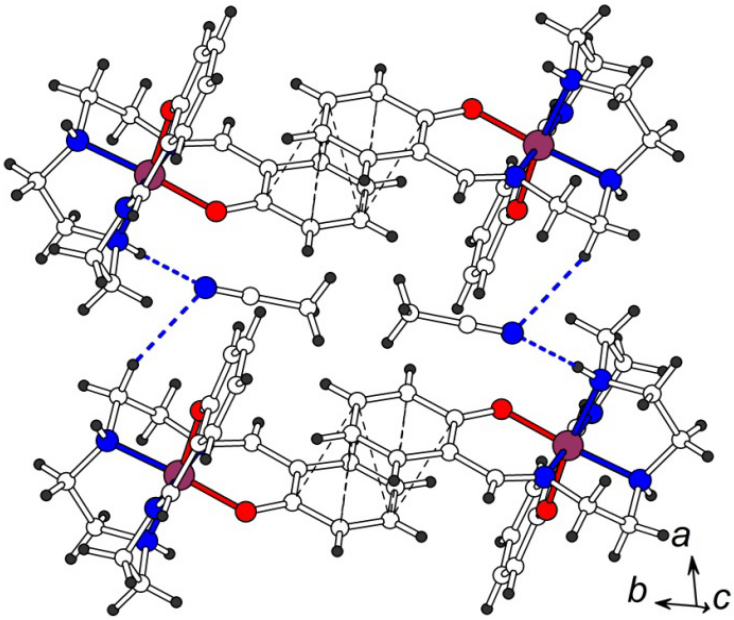

Figure S6. The $\pi\ldots\pi$ stacking in the pairs of cations in **2** (see Crystal structure section in the main text for contacts values).

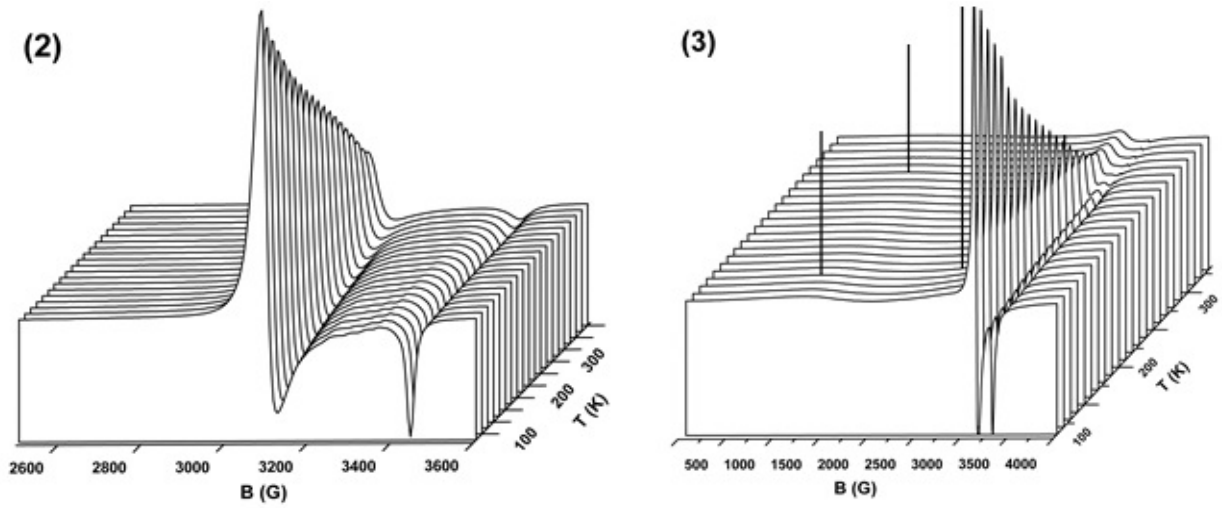

Figure S7. Temperature evolution of the EPR lineshape for **2** and **3**. Vertical lines denote position of the signal from Fe(III) ions in high-spin state (S = 5/2) in **3**.

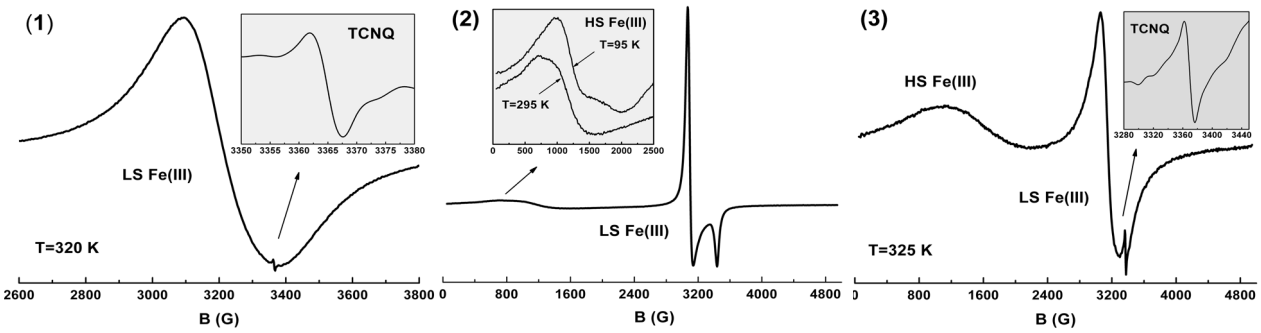

Figure S8. EPR spectra for the compounds **1**·MeOH (**1**), **2** (**2**) and **3** (**3**). A dominant line with g anisotropy in the range 1.95–2.17 belongs to Fe(III) ions in low-spin state (S = 1/2); the broad lines with g = 4.06 at 295 K, and $g_{\perp}$ = 5.6 $g_{||}$ = 3.5 at 95 K in the inset of (2), belong to Fe(III) ions in high-spin state (S = 5/2); narrow signal with g=2.005, shown in the insets of (**1**) and (**3**), belongs to anion individual radicals $TCNQ^{\bullet-}$ (S = 1/2). Concentrations of paramagnetic defects $TCNQ^{\bullet-}$ calculated relatively to that of LS Fe(III) moments at 300 K, $I_{EPR}(TCNQ^{\bullet-})/I_{EPR}$(Fe(III), are $5 \cdot 10^{-6}$ for **1**·MeOH and $3 \cdot 10^{-4}$ for **3**.

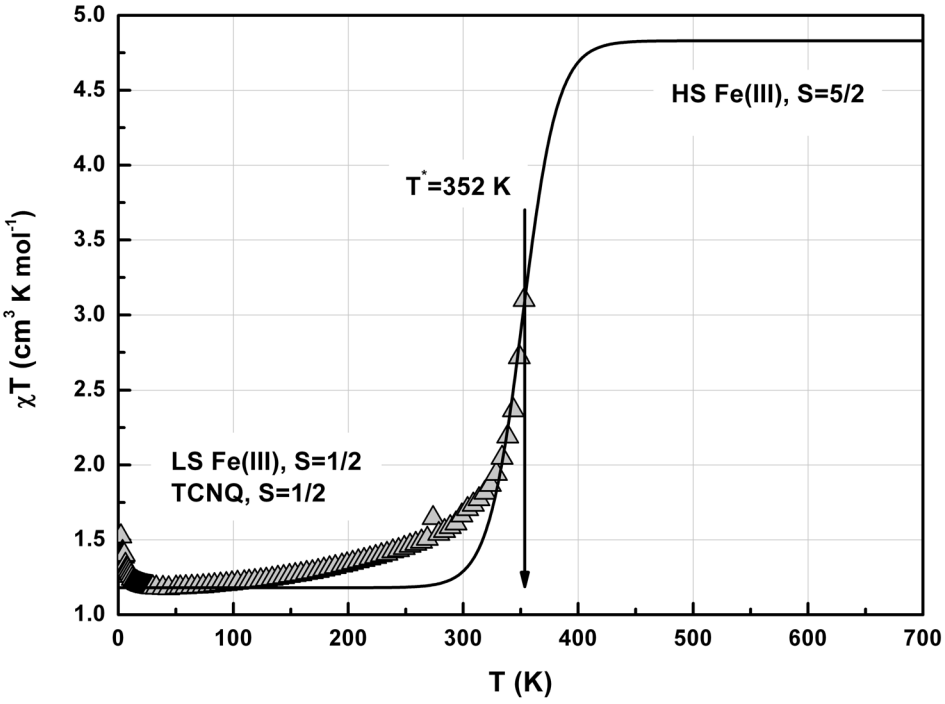

Figure S9. Evolution of the χT for **3** in the range of spin-crossover transition between the LS states, S = 1/2, and the HS states, S = 5/2, of Fe(III) ions. Solid line is a simulation by a Boltzmann distribution. A transition temperature determined at the midpoint is T^* = 355 K.

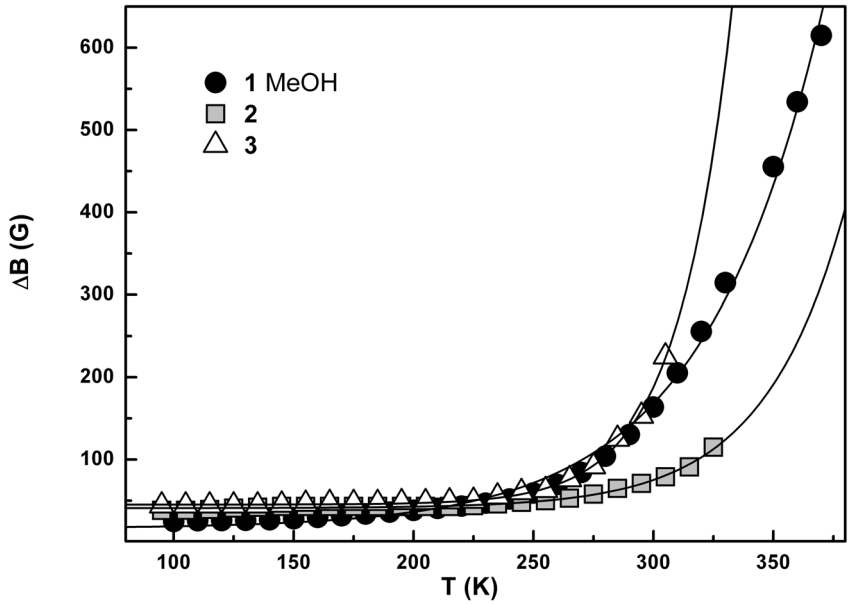

Figure S10. Best-fit curves for EPR linewidth broadening, $\Delta B(T)$, in **1**·MeOH (●), **2** (■), and **3** (Δ). Fitting function and parameters are pesented in Table S4.

Table S4. Parameters of exponential fitting curves for the EPR linewidth data in Figure S10. The fitting function is $\Delta B(T) = \Delta B_0 + A \cdot \exp(k_B T/E_a)$.

Parameter	1·MeOH	2	3
ΔB_0, G	1.62E+01	4.10E+01	4.53E+01
A, G	3.60E-01	5.00E-03	3.00E-04
E_a/k_B, K	4.96E+01	3.38E+01	2.27E+01